19th Australasian Fluid Mechanics Conference
Melbourne, Australia
8-11 December 2014

Deposition-driven Growth in Atherosclerosis Modelling

S.A. Gabriel[1], Y. Ding[1], Y. Feng[2] and J.A. Gear[1]

[1]School of Mathematical and Geospatial Sciences
RMIT University, Melbourne, Victoria 3001, Australia

[2]Mineral Resources Flagship
CSIRO, Clayton, Victoria 3169, Australia

Abstract

This study presents a preliminary analysis of atherosclerotic plaque growth as influenced by mural infiltration of low density lipoprotein (LDL). A computational model is developed to simulate physiological physics on a simplified two-dimensional bifurcating arterial geometry, comprising of a luminal volume and a wall modelled via boundary conditions. Dynamic blood flow is modelled with the incompressible Navier–Stokes equations and mass transport of LDL via passive scalar transport equations. Wall growth is modelled with explicit Lagrangian mesh motion. The modelling approach adopted in this study focuses on obtaining an estimate of the emergence and subsequent growth behaviour of atherosclerosis. For the purpose of accelerating growth, mass conservation in the growing lesion is not monitored, and in doing so, the model is made independent of a temporal scale. The purpose of this study is therefore not to obtain precise behaviour of the growing lesion, but rather an estimate at a reducing computational effort. The model is tested on a sample geometry and shown to provide a satisfactory estimate of the emergence and behaviour of atherosclerotic lesions. The findings of this study are expected to contribute to the development of more sophisticated atherosclerosis growth models which will give insight into the nature and growth behaviour of the disease.

Introduction

Atherosclerosis is a degenerative disease of arterial walls. It is characterized by the development of a protruding lesion, rich in lipids, macrophages and smooth muscle cells. Over time, progressive mass transport of lipoproteins, macrophages and smooth muscle cells, amongst other factors, contribute to the volumetric increase of the lesion, manifesting itself as a growing obstruction to the normal arterial blood flow. If left unchecked, the growing lesion may cause a significant pressure drop on the blood flow. In such a situation, the affected section of the artery becomes inefficient in transporting nutrient-carrying blood. If the pressure drop is substantially high, poor supply of oxygen to starved tissue downstream of the lesion may cause infarction. Alternatively, if the lesion significantly imposes on the blood flow, then elevated wall shear stress on its surface may cause shearing of the lesion's cap, leading to a local thrombus or the occlusion of a downstream artery. Both these outcomes will also effectively lead to ischemia of downstream tissue. If the site of infarction is significant, then the outcome may be manifest in a life-threatening disease such as stroke or myocardial infarction [7, 14, 18].

To better understand the behaviour of the disease, various mathematical models were developed by researchers to describe different aspects of atherosclerosis. An important characteristic that has of recently come under significant study, is the development of a model to capture the growth behaviour of the disease. Since growth is a multifaceted phenomenon, involving multiple co-dependent processes, such a model would require the integration of many other sub-models to collectively describe growth of the atherosclerotic lesion. To date, such models have included the transport and interaction of macromolecules and biological agents such as low density lipoproteins (LDL), oxidised LDL, cytokines, monocytes, macrophages, foam cells and smooth muscle cells, amongst others [2, 5, 6, 9, 10, 17]. These types of models considered atherosclerosis growth to be driven by mass transport mechanisms. Other models have attempted to define growth by purely mechanistic processes, as driven by arterial surface stresses defined by variations in the surrounding flow field [4, 13, 15]. This study is based on the former modelling approach, where growth is modelled as driven by mass transport. However, a relatively simplistic methodology is employed; unlike most approaches, this study does not model an arterial wall as a separate domain to that of blood flow. In doing so, no closure equations can be provided to quantitatively relate mass transport with growth. Consequently, growth cannot be related to a time scale. However, as this study only aims at investigating the spatial correlations of growth, then a temporal relation is unnecessary and so the simplifications employed are satisfactory within the scope of this study.

Model Setup

Geometry

A simplified bifurcating arterial geometry is selected for this study. Such a geometry presents intrinsic variations in cross-sectional area and in the direction of the arterial span. The combined effects of these two features on the bulk flow within the artery, causes for the formation of distinct sites with variations in wall-shear stress.

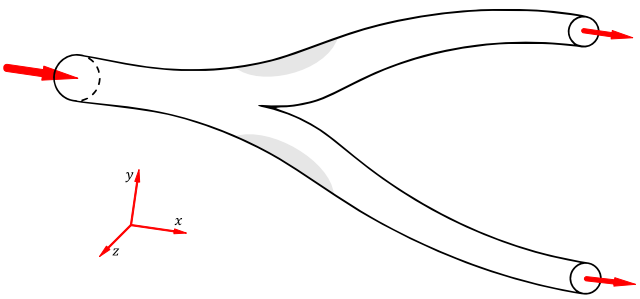

Figure 1. Outline view of a generic bifurcating artery. Shaded regions at the opposing flanks of the bifurcation are characteristic sites of oscillatory wall shear stress which promote the development of atherosclerosis.

In reference to figure 1, this study assumes a symmetric bifurcation (about the mid-plane parallel to the *x*-*z* plane). Furthermore, to restrict the study to two-dimensional flows, channel flow behaviour is assumed at the mid-plane (*x*-*y* plane) of the bifurcation. However, to enforce arterial-flow conditions, a Poiseuille boundary condition is assigned at the inlet (this is

discussed later). Additionally, to ensure the region of interest is minimally affected by the inlet and outlet boundary conditions, flow extensions are included both upstream and downstream. The resulting geometry takes the form given in figure 2.

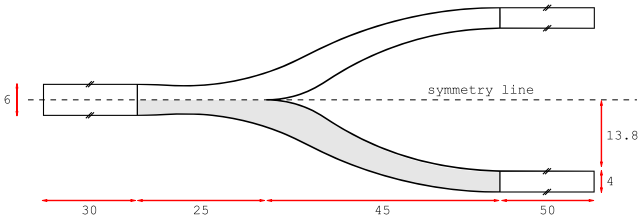

Figure 2. Geometry of computational domain of interest (shaded region) with flow extensions added; units in [*mm*].

Governing Equations

Blood flow within the arterial lumen, is described by the steady-state incompressible mass and momentum (Navier–Stokes) conservation equations respectively:

$$\nabla \cdot \boldsymbol{u} = 0 \tag{1}$$

$$\rho(\boldsymbol{u} \cdot \nabla)\boldsymbol{u} - \mu\nabla^2\boldsymbol{u} + \nabla p = 0 \tag{2}$$

Where $\boldsymbol{u}$ and p are the velocity and pressure fields respectively. Blood is assumed to be a homogenous isotropic fluid with density given by $\rho = 1050\, kg/m^3$ and viscosity by the Newtonian approximation of $\mu = 3.05 \times 10^{-3}\, kg/m/s$. The assumption that blood can be characterized by a constant viscosity is well accepted to be valid for high shear flows, typical of medium-large sized arteries [12]. However, this only holds true for the bulk flow and near-wall flow may be misrepresented by a Newtonian approximation. For the sake of simplifying the physics in this brief study, the Newtonian viscosity assumption is maintained; however it is noted that the model can be easily extended to account for more complex viscosity formulations (refer to [12] for a review of blood viscosity models).

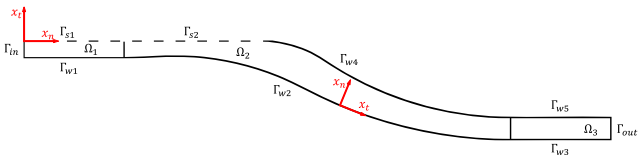

Figure 3. Boundary Γ_i and domain Ω_i labels for geometry of interest (where i is an index). Local boundary coordinate systems are described by a surface normal axis x_n and tangential axis x_t.

As atherosclerosis growth is predominantly driven by mass transport, it is important that it be included amongst the governing equations. However, as described by earlier studies such as those by Cilla et al. [5], the mass transport process involved in atherosclerosis is complex and involves multiple interacting species. Therefore for the sake of meeting the desired growth progression with modest computational resources, this study avoids the extensive modelling requirements involved by only considering mass transport of LDL from the arterial lumen into the surrounding wall. Since LDL is a dominant species involved in atherosclerosis, this approach is satisfactory for a practical estimation of expected growth sites and their subsequent behaviour. Furthermore, it is expected that due to the convection-dominated flow, small growths on an arterial wall won't significantly affect growth outcomes on the opposite wall. Therefore as this study is concerned with only one wall segment, a further simplification is made such that growth physics are applied to boundary Γ_{w2} alone (refer to figure 3) and not Γ_{w4} in the region of interest (this is discussed later).

It is well accepted that LDL is transported passively with blood flow, and so the passive scalar transport equation is employed to achieve this. For a pre-solved divergence-free vector field u and constant isotropic diffusivity D, the steady-state scalar transport equation of LDL concentration c is given by:

$$\boldsymbol{u} \cdot \nabla c - D\nabla^2 c = 0 \tag{3}$$

LDL diffusion coefficient is well accepted to be relatively constant and of the order $D = 5.0 \times 10^{-12}\, m^2/s$ in blood [19]. Concentration c is defined as a non-dimensional variable based on the inlet LDL concentration $C_0 = 1.2\, mg/mL$ [19], such that:

$$c = C/C_0 \tag{4}$$

With reference to figure 3, these governing equations are solved on all the enclosed volumetric regions Ω_i (where i is an index). The unstructured finite volume solver ANSYS Fluent is employed to solve the discretised integral forms of these equations on a computational grid of the geometry (figure 4).

At the inlet boundary Γ_{in}, a uniform concentration profile $c = 1$ is prescribed and a Poiseuille velocity profile u_n is assigned normal to the boundary:

$$u_n = 2u_{av}\left(1 - 4\left(\frac{x_t}{d}\right)^2\right) \tag{5}$$

Where d is the diameter of the whole arterial inlet and u_{av} is the average velocity derived from the Reynolds number of the flow:

$$Re = \rho u_{av} d/\mu \tag{6}$$

The equivalent non-dimensional parameter for the scalar transport equation is the mass-transfer Peclet number defined:

$$Pe = u_{av} d/D \tag{7}$$

Since the Peclet numbers of LDL species in blood flow are characteristically very large (of the order $\sim 10^8$), then effectively away from wall boundaries, concentration transport is convection-dominated. Therefore, when a steady unidirectional flow exists at the outlet, it is safe to assume a zero-flux Neumann condition at the outlet boundary [8]. Though this condition is satisfactory in the bulk flow region of the outlet, at regions near the wall it is not so due to the spatially growing mass transport boundary layer. However, since the Peclet number is large, then the transport equation is weakly elliptic and so the effects of the misrepresented near-wall outlet boundary condition is degraded away from the boundary in the upstream direction. Therefore with the addition of the flow extension downstream of the region of interest (Ω_2 in figure 3), the effects of the outlet boundary condition are not 'felt' significantly by the mass transport in Ω_2.

Due to the symmetry of the geometry (refer to figure 2), the boundaries Γ_{si} are assigned symmetry conditions in both flow and mass transport. The remaining Γ_{wi} boundaries are prescribed with no-slip wall conditions. As described earlier, the top wall regions are of no interest to this study for mass transport and surface growth (though they are necessary for the flow). Therefore, since the Peclet number is large, mass transport on the top wall Γ_{w4} won't significantly affect mass transport on the lower wall Γ_{w2}. For this reason, mass transport is ignored on the top wall and a simple Dirichlet boundary condition $c = 1$ is applied at Γ_{w4} and Γ_{w5} so that a mass boundary layer does not form. Furthermore, since Ω_1 is strictly employed as a flow extension, then to avoid a growing boundary layer on the surface Γ_{w1}, a Dirichlet boundary condition $c = 1$ is also applied there.

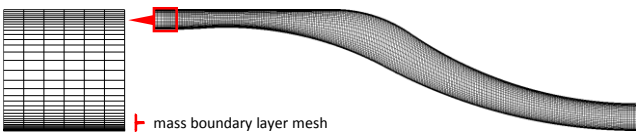

Figure 4. Meshed domain showing mass boundary layer mesh resolution.

LDL flux into the arterial wall is applied to boundaries Γ_{w2} and Γ_{w3}. It is modelled as the sum of convective flux (due to water infiltration) into the boundary and diffusive flux away from the boundary [8]; this is given by:

$$Kc_w = V_w c_w - D\frac{\partial c}{\partial x_n} \tag{8}$$

Where K is the endothelial wall's LDL permeability coefficient, V_w is the water infiltration velocity and c_w the LDL concentration at the wall surface. Water filtration is assigned a constant value of $V_w = 1.78 \times 10^{-8}\ m/s$ [16]. It is well established that wall shear stress influences endothelial mass transport and hence the formation of atherosclerosis [3, 7, 8]. LDL permeability is therefore assigned a wall shear stress (τ_w) dependence. Himburg et al. [11] established a power law correlation of the form:

$$K \propto |\tau_w|^{-0.118} \tag{9}$$

At regions of the artery where flow is not disturbed (i.e. there are no variations in wall shear stress), the endothelial permeability takes the value $K_0 = 2.0 \times 10^{-10}\ m/s$ [19]. Therefore to satisfy this condition, equation (9) is scaled to the form:

$$K = K_0\left(\frac{|\tau_{w0}|}{|\tau_w|}\right)^{0.118} \tag{10}$$

For this study, the undisturbed flow wall shear stress $|\tau_{w0}|$ is approximated by the Poiseuille flow result:

$$|\tau_{w0}| = \frac{8\mu^2}{\rho d^2}Re \tag{11}$$

Due to the boundary condition described by equation (8), a mass boundary layer is formed in the near-wall region. However, as the LDL mass-transfer Peclet number is orders of magnitude larger than the Reynolds number for the flow, the mass boundary layer formed is significantly smaller than the momentum boundary layer. For this reason, special care is required in defining the near-surface mesh, so that the mass boundary layer is well captured. A penalty of high Peclet to Reynolds number flows is therefore the excessive near-wall mesh refinement required to capture mass transfer (refer to figure 4).

Model Description

The modelling approach presented here provides an estimate of the emergence and subsequent growth of atherosclerotic lesions. This approach attempts to reduce computational effort by eliminating temporal reliance of the governing mechanics. As a consequence of this approach, modelling of a wall domain is excluded, and its effect is instead modelled with appropriate boundary conditions. This approach lacks the rigour of other models that integrate mass conservation of the growing lesion [5, 17]. However, it compensates for this by requiring considerably less computational effort. The approach presented here uses mass flux into the arterial wall as the driving force for growth. To achieve this, the wall is assumed to be an infinitely thin membrane; therefore a steady-state imbalance between mass flux entering and exiting the arterial wall is assumed to contribute to mass accumulation within the wall which would consequently drive growth. This is presented by equation (12), which describes the displacement of a material point $\boldsymbol{x}$ by accumulated mass due to LDL flux into (Kc_w) and out of (K_0c_c) the wall.

$$\boldsymbol{x}^{j+1} = \boldsymbol{x}^{j} + f_g \max\left\{\frac{Kc_w - K_0c_c}{K_0c_c}\ ,\ 0\right\}\boldsymbol{n} \tag{12}$$

The wall's out-flux is taken to be equivalent to an in-flux condition at normal flow permeability K_0 and critical concentration of $c_c = 1.2$. Since flow and mass transport are solved to steady-state, a time scale is not involved. Alternatively, an iterative procedure as described by figure 5 is employed. To reduce the number of iterations performed and effectively accelerate growth, a multiplicative factor f_g is proposed such that the resulting displacement is large enough to critically affect the local surface normal $\boldsymbol{n}$ but not the flow field. Therefore, N_j iterations are performed to update the local surface mesh until the accumulated displacement is critically sufficient to influence the flow field since the last i-iteration. Following this, the flow and mass transport equations are resolved, and the procedure iterated N_i times. The parameter N_j is therefore a function of the mesh length scales and the minimum length scale that would influence the flow; the smaller the parameter, the better the approximation. Whereas N_i is determined by the user's preference and is comparable to the total time of growth.

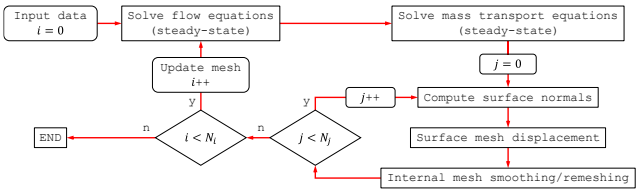

Figure 5. Growth modelling algorithm.

Results and Discussion

The algorithm presented in figure 5 with the equations described earlier are implemented into ANSYS Fluent v14.5. For this study, Reynolds numbers characteristic of medium-large sized arteries are assessed for their influence on the emergence and growth behaviour of atherosclerotic lesions. The algorithm's iteration parameters are selected to be $N_i = 20$ and $N_j = 50$. The results for this study are presented in figure 6 for a Reynolds number range $Re = \{150, 300, 450, 600\}$.

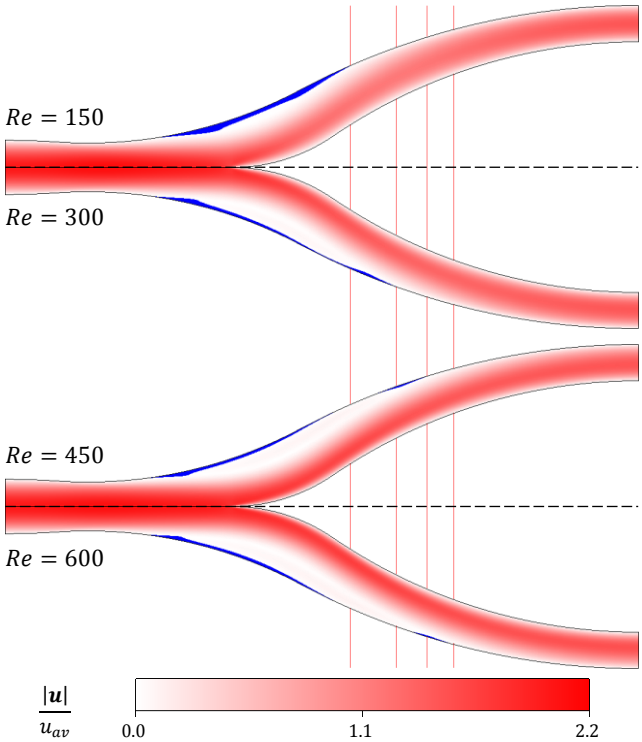

Figure 6. Wall growth results (blue) at $N_i = 20$ for four Reynolds numbers. The surrounding luminal flow velocity distribution is presented in non-dimensional form. Note, geometries are stacked about symmetry line for purpose of illustrating the arterial bifurcation (4 separate cases).

From the flow distribution in figure 6, it is noticeable that the non-dimensional flow velocity takes a similar magnitude and pattern distribution in the bulk flow for each Reynolds number

tested. A distinctive variance is noticeable, mainly in the size of the recirculation zone formed at the flanks of the bifurcating site. It is well known [1] and shown in figure 6, that a direct relationship exists between flow Reynolds number and recirculation zone size. Implied from this is that at higher Reynolds numbers, larger low wall shear stress zones would form and so regions with high LDL flux into the arterial wall will be more distributed. This is noticeable in the distribution of growth lesions in figure 6; with higher Reynolds number flow, lesions are spread over larger space.

It is observed that the extent of variation in the distribution of growth lesions is more pronounced at regions near the end of the recirculation zone than at the start. This is made evident by the vertical lines in figure 6, which mark the ends of the growth lesions for each Reynolds number case. This result is explained to be due to the geometry, which strongly influences the site of emergence of recirculation zones, whereas flow Reynolds number influences their size.

With the same settings and iterations applied to each Reynolds number case, it is noticeable that the extent of growth normal to the surface is less pronounced for high Reynolds number flow. It is noticeable that though lesions are more spread out, they are thinner at high Reynolds numbers. This can be explained to be due to higher convective flow at the near-wall regions, which would reduce the diffusive flux term in equation (3), causing the mass transport boundary layer to be smaller and effectively reduce mass flux into the arterial wall (refer to equation (8)).

Conclusions

This study presents a computational model, designed with the intention to provide an estimate of the emergence and subsequent growth behaviour of atherosclerotic lesions. The developed model attempts to ease computational requirements by eliminating a time scale and reducing the number of species involved in mass transport to just that of LDL. Furthermore the arterial wall is eliminated as a separate domain, and its effect is instead modelled via boundary conditions. The model is assessed on a bifurcating arterial geometry and shown to provide a satisfactory estimate of the emergence and subsequent growth behaviour of atherosclerotic lesions. The results obtained were shown to correlate strongly with variations in Reynolds number, indicating the importance of resolving accurate flow fields in the development of atherosclerosis growth models.

Acknowledgments

This research was supported by an Australian Postgraduate Award and a grant from the CSIRO. The authors wish to also thank LEAP Australia for providing technical support with the ANSYS Fluent software package.

References

[1] Armaly, B.F., Durst, F., Pereira, J.C.F. & Schönung, B., Experimental and theoretical investigation of backward-facing step flow, *Journal of Fluid Mechanics*, **127**, 1983, 473-496.

[2] Calvez, V. et al., Mathematical and numerical modeling of early atherosclerotic lesions, *ESAIM: Proceedings*, **30**, 2010, 1-14.

[3] Cecchi, E. et al., Role of hemodynamic shear stress in cardiovascular disease, *Atherosclerosis*, **214**, 2011, 249-256.

[4] Chen, C.X., Ding, Y. & Gear, J.A., Numerical simulation of atherosclerotic plaque growth using two-way fluid-structural interaction, *The ANZIAM Journal*, **53**, 2012, 278-291.

[5] Cilla, M., Peña, E. & Martínez, M.A., Mathematical modelling of atheroma plaque formation and development in coronary arteries, *Journal of the Royal Society, Interface*, **11**, 2014, 1-16.

[6] Díaz-Zuccarini, V., Di Tomaso, G., Agu, O. & Pichardo-Almarza, C., Towards personalised management of atherosclerosis via computational models in vascular clinics: technology based on patient-specific simulation approach, *Healthcare Technology Letters*, **1**, 2014, 13-18.

[7] Douglas, G. & Channon, K.M., The pathogenesis of atherosclerosis, *Medicine*, **38**, 2010, 397-402.

[8] Ethier, C.R., Computational Modeling of Mass Transfer and Links to Atherosclerosis, *Annals of Biomedical Engineering*, **30**, 2002, 461-471.

[9] Filipovic, N. et al., Computer simulation of three-dimensional plaque formation and progression in the carotid artery, *Medical & Biological Engineering & Computing*, **51**, 2013, 607-616.

[10] Gessaghi, V.C. et al., Growth model for cholesterol accumulation in the wall of a simplified 3D geometry of the carotid bifurcation, *Computer Methods in Applied Mechanics and Engineering*, **200**, 2011, 2117-2125.

[11] Himburg, H.A. et al., Spatial comparison between wall shear stress measures and porcine arterial endothelial permeability, *American journal of physiology. Heart and circulatory physiology*, **286**, 2004, 1916-1922.

[12] Johnston, B.M., Johnston, P.R., Corney, S. & Kilpatrick, D., Non-Newtonian blood flow in human right coronary arteries: steady state simulations, *Journal of biomechanics*, **37**, 2004, 709-720.

[13] Kuhl, E., Maas, R., Himpel, G. & Menzel, A., Computational modeling of arterial wall growth. Attempts towards patient-specific simulations based on computer tomography, *Biomechanics and modeling in mechanobiology*, **6**, 2007, 321-331.

[14] Libby, P., Atherosclerosis: the new view, *Scientific American*, **286**, 2002, 46-55.

[15] Liu, B. & Tang, D., Computer simulations of atherosclerotic plaque growth in coronary arteries, *Molecular & cellular biomechanics*, **7**, 2010, 193-202.

[16] Meyer, G., Merval, R. & Tedgui, A., Effects of pressure-induced stretch and convection on low-density lipoprotein and albumin uptake in the rabbit aortic wall, *Circulation research*, **79**, 1996, 532-540.

[17] Silva, T., Sequeira, A., Santos, R.F. & Tiago, J., Mathematical Modeling of Atherosclerotic Plaque Formation Coupled with a Non-Newtonian Model of Blood Flow. *Conference Papers in Mathematics*, 2013, 1-14.

[18] Slager, C.J. et al., The role of shear stress in the destabilization of vulnerable plaques and related therapeutic implications, *Nature clinical practice. Cardiovascular medicine*, **2**, 2005, 456-64.

[19] Stangeby, D.K. & Ethier, C.R., Computational analysis of coupled blood-wall arterial LDL transport, *Journal of biomechanical engineering*, **124**, 2002, 1-8.